

**REUSABILITY OF ZINC OXIDE NANOROD FOR PHOTOCATALYTIC
DECOMPOSITION OF RHODAMINE B DYE AFTER COPPER METAL
DEPOSITION**

by

LE ANH THI

**Thesis submitted in fulfillment of the
requirements for the degree of
Master of Science**

December 2018

ACKNOWLEDGEMENT

First and foremost, I would like to express my deepest appreciation to my main supervisor, Assoc. Prof. Ir. Dr. Pung Swee Yong and co-supervisor, Prof. Ir. Dr. Srimala A/P Sreekantan for the supports and motivations to complete my master research project. Without their guidance and persistent help, this thesis would not have been possible.

Next, I would like to acknowledge to the Ministry of Higher Education, Malaysia under Fundamental Research Grant Scheme (FRGS) (Grant No. 203.PBAHAN.6071327) and AUN/SEED Net under Collaborative Research Program (CR) (Grant No. 304.PBAHAN.6050354) for providing the research funding to conduct my master program.

I also would like to express my gratitude to Dean, School of Materials and Mineral Resources Engineering (SMMRE) of Universiti Sains Malaysia (USM) for providing me a safety environment and research facilities. Many thanks to lecturers, technicians and administrative staffs of SMMRE for their great helps in the utilization of equipment as well as supports and recommendations in problems solving to complete my master research project.

Last but not least, special thanks to my postgraduate friends and seniors who are willing to discuss and support me throughout my study at USM.

TABLE OF CONTENTS

	Page
ACKNOWLEDGEMENT	ii
TABLE OF CONTENTS	iii
LIST OF TABLES	vi
LIST OF FIGURES	vii
LIST OF ABBREVIATIONS	xii
LIST OF SYMBOLS	xiii
ABSTRAK	xiv
ABSTRACT	xvii
CHAPTER ONE: INTRODUCTION	
1.1 Research background	1
1.2 Problem statement	3
1.3 Research objectives	4
1.4 Scope of the study	5
CHAPTER TWO: LITERATURE REVIEW	
2.1 Water pollution	7
2.2 Organic dyes pollutants	8
2.2.1 Classification	8
2.2.2 Impact of organic dye pollutants	9
2.2.3 Methods of dye removal	9
2.3 Inorganic pollutants	12
2.3.1 Classification	12
2.3.2 Impact of heavy metal pollutant	12
2.3.3 Methods of heavy metal removal	13
2.4 Semiconductor photocatalysis	14
2.4.1 Applications	15
2.4.2 Fundamental of ZnO photocatalyst	25
2.4.3 Synthesis of ZnO nanostructures	26
2.4.4 Crystal structure and optical properties of ZnO	31

CHAPTER THREE: MATERIALS AND RESEARCH METHODOLOGY

3.1	Introduction	35
3.2	Raw materials and chemicals	35
3.3	Synthesis ZnO NRs and ZnO NDs	38
3.4	Photocatalytic study in organic dyes removal	39
3.5	Heavy metal removal study	40
3.6	Photodegradation of RhB dye by M/ZnO hybrid particles	40
3.7	Characterization techniques	41
3.7.1	X-ray Dispersive spectroscopy (XRD)	41
3.7.2	Fourier Transform Infrared Spectroscopy (FTIR)	41
3.7.3	Field Emission Scanning Electron Microscope/Energy Diffraction X-ray (FESEM/EDX)	41
3.7.4	High Resolution Transmission Electron Microscope (HRTEM)	42
3.7.5	UV-Visible spectroscopy	42
3.7.6	Inductively Coupled Plasma – Optical Emission Spectrometry (ICP-OES)	43
3.7.7	Zeta potential analysis	43

CHAPTER 4: RESULTS AND DISCUSSION

4.1	Introduction	44
4.2	Synthesis and characterization of ZnO NRs and ZnO NDs	44
4.2.1	Structural and optical properties	44
4.2.2	Growth mechanism	51
4.3	Photocatalytic study of ZnO NRs and ZnO NDs	52
4.3.1	Characterization of Rhodamine B (RhB)	52
4.3.2	Photocatalytic study of ZnO NRs and ZnO under NDs visible light illumination	53
4.3.3	Photocatalytic study of ZnO NRs and ZnO NDs under UV light illumination	56
4.3.4	Scavenger study of ZnO NRs and ZnO NDs	59
4.3.5	Photodegradation mechanism of RhB dye	62
4.4	Heavy metal ions removal by ZnO NRs	64

4.4.1	Removal efficiency of heavy metal ions by of ZnO NRs	64
4.4.2	Structural and optical properties of M/ZnO hybrid particles	69
4.4.3	Heavy metal ions removal mechanisms by ZnO NRs under UV exposure	83
4.5	Reusability of M/ZnO hybrid particles in photodegradation of RhB dye	91
CHAPTER FIVE: CONCLUSION		
5.1	Conclusions	100
5.2	Recommendations for future work	101
REFERENCES		103
LIST OF PUBLICATIONS		

LIST OF TABLES

		Page
Table 2.1	Photodegradation of organic dyes in aqueous solution of ZnO particles	18
Table 2.2	Table 2.2 Photodegradation mechanism of dyes pollutant under UV and visible light	20
Table 2.3	Heavy metal removal using semiconductor photocatalysts	24
Table 2.4	Synthesis methods of ZnO	30
Table 3.1	The formula, molecular weight, function and supplier of chemical used in this study	37
Table 4.1	Possible removal mechanism of heavy metal ions removal by ZnO NRs	68
Table 4.2	Deposition of metal/metal oxide onto the surface of ZnO NRs under UV irradiation and their removal mechanisms	85
Table 4.3	Coefficient of linear line (R^2) of RhB in the solution of ZnO NRs, M/ZnO hybrid particles under UV irradiation	94
Table 4.4	Coefficient of linear line (R^2) of RhB in the solution of ZnO NRs, M/ZnO hybrid particles under visible irradiation	97

LIST OF FIGURES

		Page
Figure 2.1	Structure of Rhodamine B (RhB) dye	8
Figure 2.2	Band gap energy, VB and CB for a range of semiconductors on a potential scale (V) versus the normal hydrogen electrode (NHE)	14
Figure 2.3	Absorbance spectra of RhB solution degraded by stacked ZnO nanorods under UV light irradiation	16
Figure 2.4	The photocatalytic mechanism of organic dye degradation under (a) UV and (b) visible light illumination	21
Figure 2.5	Position of the redox potentials of various metallic couples and oxidation potentials of water related to the energy levels vs. NHE of ZnO photocatalyst	23
Figure 2.6	Schematic illustration of TiO ₂ application in arsenic removal	25
Figure 2.7	Preferential growth direction of ZnO wurzite crystal and possible structure	26
Figure 2.8	Morphology of ZnO particles synthesized by different methods	27
Figure 2.9	FTIR spectrum of ZnO particles	29
Figure 2.10	ZnO crystal structure (a) cubic rocksalt, (b) cubic zinc blende, and (c) hexagonal wurtzite. Shaded gray and black spheres denote Zn and O atoms, respectively	31
Figure 2.11	XRD patterns of ZnO nanoparticles: (a) standard XRD pattern and (b) sample XRD pattern	32
Figure 2.12	(a) 2-D EDX mapping of ZnO nanoflowers, (b) EDS spectrum and quantitative composition of ZnO. (c) XRD pattern of Zn and ZnO NCs. (d) TEM micrograph of a ZnO nanorod; the left panel is the TEM image of the ZnO nanorod, and the inset is the SAED pattern obtained along the [110] direction; the centre and right panels are the HRTEM image	33
Figure 2.13	a) Optical band gap of ZnO; b) Diffuse Reflectance Spectra of synthesized ZnO	34
Figure 3.1	Flow chart of the project	36

Figure 4.1	XRD patterns of (a) ZnO NRs, (b) ZnO NDs, (c) ZnO JCPDS No. 98-002-7791 and (d) ZnAlOHCO ₃ JCPDS No. 98-010-5856	45
Figure 4.2	EDX analysis (b) SEM image of ZnO NRs synthesized using Zinc nitrate tetrahydrate, PVP and Hexamine	46
Figure 4.3	TEM image, (b) SAED, (c) HRTEM and EDX mapping of (d) zinc and (e) oxygen in ZnO NRs	46
Figure 4.4	SEM image (b) EDX analysis of ZnO NDs synthesized using Zinc acetate dehydrate, ammonia hydroxide and Aluminium sulphate	47
Figure 4.5	(a) TEM, (b) SAED, (c) HRTEM and EDX mapping of (d) zinc, (e) oxygen and (f) aluminium in ZnO NDs	48
Figure 4.6	The FTIR spectra of (a) ZnO NRs and (b) ZnO NDs	49
Figure 4.7	(a) Room temperature UV-visible diffuse reflectance spectra and (b) band gap energy value of ZnO NRs and ZnO NDs	49
Figure 4.8	Zeta potential of (a) ZnO NRs and (b) ZnO NDs	50
Figure 4.9	(a) Characteristic absorption spectra and (b) structure of Rhodamine B (RhB)	52
Figure 4.10	Typical UV-Vis spectrum profile of RhB dye during the illumination of the (a) UV light, (b) visible light and (c) photodegradation efficiency of RhB dye in the aqueous system	53
Figure 4.11	Absorption peak of RhB in aqueous solution of (a) ZnO NRs, (b) ZnO NDs, (c) photodegradation efficiency and (d) photodegradation rate under visible light irradiation	55
Figure 4.12	Blue shift of the absorption peak of RhB dye in the photodegradation process of ZnO NRs and ZnO NDs under visible illumination	56
Figure 4.13	Absorbance spectra of RhB dye in solution of (a) ZnO NRs, (b) ZnO NDs (c) photodegradation efficiency and (d) discoloration rate of RhB dye under UV light irradiation	57
Figure 4.14	Blue shift of absorbance peak of RhB dye solution containing ZnO NRs and ZnO NDs under UV light irradiation	58

Figure 4.15	(a) Photodegradation efficiency after 5 hours of irradiation, (b) rate constant of degradation of RhB solution under UV light and visible light irradiation in the presence and absence of ZnO NRs and ZnO NDs	59
Figure 4.16	Scavenger test (a) photodegradation efficiency and (b) rate constant of degradation of RhB dye by ZnO NRs under visible light irradiation	60
Figure 4.17	Scavenger test (a) photodegradation efficiency and (b) rate constant of degradation of RhB dye by ZnO NDs under visible light irradiation	60
Figure 4.18	Scavenger test (a) photodegradation efficiency and (b) rate constant of degradation of RhB dye by ZnO NRs under UV light irradiation.	61
Figure 4.19	Scavenger test (a) photodegradation efficiency and (b) rate constant of degradation of RhB dye by ZnO NDs under UV light irradiation.	61
Figure 4.20	Photocatalytic removal of heavy metal ions in ZnO NRs suspension exposing under (a) UV light, (b) visible light and (c) without light. Initial metal concentration: 50 ppm, concentration of ZnO 1g/l, pH = 6.5-7, temperature 25 ⁰ C	65
Figure 4.21	Removal efficiency of heavy metal ions in ZnO NRs suspension exposing under (a) UV light, (b) visible light and (c) dark condition	66
Figure 4.22	Removal efficiency of Ag, Cr, Pb, Mn, Cu, Cd and Ni after 60 min irradiation of UV, visible light and dark condition in the aqueous solution of ZnO NRs	68
Figure 4.23	XRD spectra of (a) ZnO NRs, (b) Ag/ZnO, (c) Cr/ZnO, (d) Pb/ZnO, (e) Mn/ZnO, (f) Cu/ZnO, (g) Cd/ZnO, (h) Ni/ZnO hybrid particles. The deposition of heavy metals were carried out under UV light irradiation.	69
Figure 4.24	XRD spectra of (a) ZnO NRs, (b) Ag/ZnO, (c) Cr/ZnO, (d) Pb/ZnO, (e) Mn/ZnO, (f) Cu/ZnO, (g) Cd/ZnO, (h) Ni/ZnO hybrid particles. The deposition of heavy metals were carried out under visible light irradiation.	70
Figure 4.25	SEM image of (a) Ag/ZnO, (b) Cr/ZnO, (c) Pb/ZnO, (d) Mn/ZnO, (e) Cu/ZnO, (f) Cd/ZnO and (g) Ni/ZnO hybrid particles after removal of heavy metal ions under UV light irradiation	74

Figure 4.26	SEM image of (a) ZnO, (b) Ag/ZnO, (c) Cr/ZnO, (d) Pb/ZnO, (e) Mn/ZnO, (f) Cu/ZnO, (g) Cd/ZnO and (h) Ni/ZnO hybrid particles after removal of heavy metal ions under visible light irradiation	76
Figure 4.27	(a) TEM image; (b) HRTEM image and EDX mapping of (c) Zn, (d) O and (e) Ag element of ZnO particles after the removal of Ag(I) under UV irradiation.	77
Figure 4.28	(a) TEM image; (b) HRTEM image and EDX mapping of (c) Zn, (d) O and (e) Cr element of ZnO particles after the removal of Cr(VI) under UV irradiation.	78
Figure 4.29	(a) TEM image; (b) HRTEM image and EDX mapping of (c) Zn, (d) O and (e) Pb element of ZnO particles after the removal of Pb(II) under UV irradiation.	79
Figure 4.30	(a) TEM image; (b) HRTEM image and EDX mapping of (c) Zn, (d) O and (e) Mn element of ZnO particles after the removal of Mn(II) under UV irradiation.	80
Figure 4.31	(a) TEM image; (b) HRTEM image and EDX mapping of (c) Zn, (d) O and (e) Cu element of ZnO particles after the removal of Cu(II) under UV irradiation.	80
Figure 4.32	(a) TEM image; (b) HRTEM image and EDX mapping of (c) Zn, (d) O and (e) Cd element of ZnO particles after the removal of Cd(II) under UV irradiation.	81
Figure 4.33	(a) TEM image; (b) HRTEM image and EDX mapping of (c) Zn, (d) O and (e) Ni element of ZnO particles after the removal of Ni(II) under UV irradiation.	82
Figure 4.34	Diffusion reflectance of Ag/ZnO, Cr/ZnO, Pb/ZnO, Mn/ZnO, Cu/ZnO, Cd/ZnO, Ni/ZnO hybrid particles obtained in the process of UV illumination	83
Figure 4.35	Mechanism of heavy metal ions removal using ZnO NRs via reduction process	87
Figure 4.36	Mechanism of heavy metal ions removal using ZnO NRs via oxidation process	88
Figure 4.37	Absorbance peaks of RhB in the aqueous suspension of (a) Ag/ZnO, (b) Cr/ZnO, (c) Pb/ZnO, (d) Mn/ZnO, (e) Cu/ZnO, (f) Cd/ZnO and (g) Ni/ZnO hybrid particles under UV irradiation	92
Figure 4.38	(a) Photodegradation efficiency within 5 hours, (b) degradation efficiency at 1 hour (c) degradation rate and	93

	(d) rate constant of degradation of RhB by M/ZnO hybrid particles under UV irradiation	
Figure 4.39	Photocatalytic mechanisms in RhB dye removal by various configuration of ZnO hybrid particles: (a) ZnO particles, (b) MO _x /ZnO hybrid particles and (c) M/ZnO hybrid particles. (M: metal ion)	96
Figure 4.40	Absorbance peak of RhB in the aqueous suspension of (a) Ag/ZnO, (b) Cr/ZnO, (c) Pb/ZnO, (d) Mn/ZnO, (e) Cu/ZnO, (f) Cd/ZnO and (g) Ni/ZnO hybrid particles under visible irradiation	98
Figure 4.41	(a) Photodegradation efficiency, (b) Maximum of photodegradation efficiency, (c) degradation rate after 3 hours of irradiation and (c) rate constant of degradation of RhB in aqueous solution of M/ZnO hybrid particles under visible irradiation	99

LIST OF ABBREVIATIONS

AOP	Advanced oxidation process
CB	Conduction band
DOE	Department of Environment Malaysia
EDX	Energy-Dispersive X-ray
FESEM	Field Emission Scanning Electron Microscope
HRTEM	High Resolution Transmission Electron Microscope
ICP-OES	Inductively Coupled Plasma – Optical Emission Spectrometry
JCPDS	Joint Committee on Powder Diffraction Standards
M	Metals
NDs	Nanodisks
NHE	Normal hydrogen electrode
NPs	Nanoparticles
NRs	Nanorods
PL	Photoluminescence
RhB	Rhodamine B
ROS	Reactive oxygen species
SAED	Selected Area Electron Diffraction
TEM	Transmission Electron Microscope
UV	Ultraviolet
VB	Valence band
WHO	World Health Organization
XRD	X-Ray Diffraction

LIST OF SYMBOLS

%	Percentage
μm	Micrometre
$^{\circ}\text{C}$	Degree Celsius
eV	Electron Volt
g	Gram
m^3	Cubic meter
mg/l	Milligram per litter
mL	Milliliter
nm	Nanometre
ppm	Part per million

**PENGGUNAAN SEMULA ROD NANO OKSIDA ZINK UNTUK
FOTOMANGKIN DALAM PEMBUANGAN PENCELUP ORGANIK
RHODAMINE B SELEPAS PENGENDAPAN LOGAM KUPRUM**

ABSTRAK

Proses oksidasi termaju yang terdiri daripada fotomangkin semikonduktor merupakan kemunculan teknik untuk rawatan air kumbahan. Walau bagaimanapun, kadar hayat semikonduktor fotomangkin ini masih lagi di dalam kajian. Selepas pembuangan logam berat, tapak pemangkin yang paling aktif telah dihalang oleh logam berat. Justeru, ia memberi kesan yang berbeza pada prestasi fotomangkin di dalam pembuangan pencelup organik. Dalam kajian ini, rod nano ZnO dan disk nano ZnO telah disintesis melalui teknik pemendakan dan menilai aktiviti fotomangkin dalam degradasi pencelup Rhodamine B (RhB) selepas pengendapan logam berat. Purata panjang dan diameter rod nano ZnO masing-masing adalah 497.34 ± 15.55 nm dan 75.78 ± 10.39 nm. Disk nano ZnO menunjukkan purata diameter iaitu 2.12 ± 0.39 μ m dan ketebalan 74.91 ± 17.67 nm. Fotodegradasi pencelup RhB oleh zarah ZnO juga didapati mengikut tindakbalas kinetik tertib-pertama. Rod nano ZnO berkesan menyerap ion-ion logam berat seperti Cu(II), Ag(I) dan Pb(II) dengan kecekapan masing-masing 100%, 97.92% and 85.18% di bawah pendedahan cahaya UV selama 1 jam. Walau bagaimanapun, penyerapan yang kurang cekap telah diperlihatkan oleh Cr(VI), Mn(II), Cd(II) dan Ni(II) masing-masing iaitu 14.83%, 8.62%, 7.23% and 4.76%. Ion-ion logam berat ini telah ditukarkan kepada logam-logam atau logam oksida melalui reduksi/oksidasi atau mekanisma penyerapan. Kecekapan degradasi pewarna RhB oleh Cu/ZnO, Ag/ZnO, Mn/ZnO, Cd/ZnO dan zarah-zarah hybrid Ni/ZnO didapati lebih baik berbanding zarah ZnO tetapi tidak pada kes zarah-zarah hybrid Pb/ZnO and Cr/ZnO. Secara kesimpulannya, rod nano ZnO menunjukkan

kebolehan yang luar biasa untuk mengdegradasi pewarna RhB di bawah radiasi cahaya UV selepas pemendapan logam berat.

REUSABILITY OF ZINC OXIDE NANOROD FOR PHOTOCATALYTIC DECOMPOSITION OF RHODAMINE B DYE AFTER COPPER METAL DEPOSITION

ABSTRACT

Advanced oxidation process based on semiconductor photocatalysts is an emerging technique for wastewater treatment. However, the lifetime of these semiconductor photocatalysts is yet to be fully studied. After heavy metal removal, most active sites of catalyst are blocked by heavy metal. Therefore, it affects the subsequent photocatalytic performance differently in organic dye removal. In this work, ZnO nanorods (NRs) and nanodisks (NDs) were synthesized by precipitation method and evaluate the photocatalytic activity to degrade Rhodamine B dye after heavy metal deposition. The average length and diameter of ZnO NRs were 497.34 ± 15.55 nm and 75.78 ± 10.39 nm, respectively. The ZnO NDs have average diameter of 2.12 ± 0.39 μ m and thickness of 74.91 ± 17.67 nm. The photodegradation of RhB dye by ZnO particles followed first-order kinetic reaction. ZnO NRs removed effectively heavy metal ions such as Cu(II), Ag(I) and Pb(II) ions with efficiency of 100%, 97.92% and 85.18%, respectively under exposure of UV light for 1 hour. However, poor removal efficiency, i.e. 14.83%, 8.62%, 7.23% and 4.76%, respectively was observed for Cr(VI), Mn(II), Cd(II) and Ni(II). These heavy metal ions were removed in the forms of metals or metal oxide via reduction/oxidation or adsorption mechanisms. The degradation efficiencies of RhB dye by Cu/ZnO, Ag/ZnO, Mn/ZnO, Cd/ZnO and Ni/ZnO hybrid particles were better than ZnO particles but not the case of Pb/ZnO and Cr/ZnO hybrid particles. In conclusion, the ZnO NRs in general showed a remarkable ability to degrade RhB dye under UV irradiation after heavy metal deposition.

CHAPTER ONE

INTRODUCTION

1.1 Research background

The common pollutants found in water are inorganic and organic compounds. Examples of inorganic compounds are heavy metal ions. These heavy metal ions are discharged to the environment from various activities such as agricultural, electroplating, metal finishing, painting, mining and fossil fuel. Supply water resources, including surface water and ground water, may get contaminated by these heavy metal wastes. Long term excessive ingestion of these metals by human could damage kidney, liver, brain function, nervous system or even death (Barakat, 2011).

In addition to heavy metal contaminants, organic pollutants were found in the wastewater. One of the major contributors of organic pollutants is textile manufacturing. In fact, the textile dyeing and finishing processes are estimated to be the source of 17 to 20 percents of industrial water pollution. The dyes commonly used in these industries are Rhodamine B (RhB), Rhodamine 6G, methyl orange and methylene blue. These persistent organic dyes are difficult to decompose in nature due to its chemical stability. The release of these untreated dyes into the water systems causes a serious health concern. Textile effluent is one of the causes of environment issues and human illnesses. It is estimated that 40 percent of globally used organic dyes contain chlorine which cause skin irritation, allergic reaction and may harm to children (Kant, 2012).

Various treatment techniques have been applied for the removal of inorganic and organic contaminant from wastewater such as chemical treatment (Al-Shannag et al., 2015; Brillas & Martínez-Huitle, 2015), adsorption (Abbas et al., 2016; Yu et al.,

2014), filtration technology (Hebbar et al., 2016; Kebria et al., 2015), ion exchange (Zewail & Yousef, 2015) and photocatalysis technique (Jiang et al., 2012). Among these techniques, photocatalysis process based on semiconductor materials has been paid much attention as complementary technique in the degradation of organic dyes as well as heavy metal ions removal.

The common used semiconductor as photocatalyst are TiO_2 (Litter, 2015; Khan et al., 2015a) and ZnO (Ong et al., 2018; Pung et al., 2012) because of their wide band gap energy level, which is able to generate several reactive species. Therefore, semiconductor photocatalyst can be used for the degradation of organic dyes (Seo & Shin, 2015; Asiri et al., 2011; Tripathy et al., 2017) and the removal of toxic metal ions (Wahyuni et al., 2015; Rahimi et al., 2014; Joshi & Shrivastava, 2011; Barakat et al., 2004; Shirzad Siboni et al., 2011). The photocatalysis process has a number of advantages, including high removal efficiency and self-generated reactive species, etc. The oxidation processes do not require expensive oxidizing chemicals as compared to other advance technology such as hydrogen peroxide and ozone (Anandan et al., 2010a).

The photocatalyst process occurs when semiconductor absorbs the energy (light) that equal or higher than its band gap energy. Then the electrons in the occupied valance band (VB) are excited to conduction band (CB) and leave the positive hole in the VB. These charge carriers react with donors or acceptors that adsorbed on the surface of the photocatalyst, producing reactive oxygen species such as hydroxyl radical ($\cdot\text{OH}$) and superoxide radical ($\cdot\text{O}_2^-$) in the liquid interface. These radical ions are responsible for the oxidation of organic dyes into less toxic substances. In contrary, the free generated electrons are able to reduce the heavy metal ion (M^+) to metal and deposited on the surface of semiconductor material (Anandan et al., 2010b).

1.2 Problem statement

ZnO has been chosen as a photocatalyst in this work due to its high catalyst efficiency, low cost, large bandgap (3.37 eV) and nontoxic nature. In recent study, it has been shown that ZnO was more effective than TiO₂ in organic pollutants removal (Sil & Chakrabarti, 2010; Sakthivel et al., 2003). Difference morphology of ZnO nanostructures (e.g. nanorod, nanodisk, nanowire, nanosheet, nanoflower, etc.) could be obtained by adjusting the synthesis parameters. These nanostructures might affect the photocatalytic performance of ZnO catalyst in the degradation of organic dyes differently attributed to its different exposed crystal planes. It is noted that ZnO crystal has strong tendency to grow along the [0001] direction (Leonardi, 2017). Thus, the most commonly found ZnO nanostructures is ZnO nanorods (NRs).

On the other hand, ZnO nanodisks (NDs) possess unique characteristic as the disk surface is either consists of negatively charge (-O) terminated or positively charge (-Zn) terminated. This large polar surface area might affect the photocatalytic performance of ZnO in photodegradation of organic pollutants and removal of heavy metals. Thus, both ZnO nanostructures were selected in this project. In addition, Rhodamine B (RhB) dye was used in this project due to its severe ecological impact. It is crucial to investigate the photocatalytic activity of ZnO NRs and ZnO NDs for the degradation of RhB dye.

The wastewater contains mixture of unknown inorganic and organic pollutants. Since heavy metal ions are hazard for human and environment, efforts for removal the heavy metal ions by ZnO photocatalyst have attracted much attention. As reported in the literature, most researchers have focused on the reduction of toxic Cr(VI) by using ZnO photocatalyst (Qamar et al., 2011; Joshi & Shrivastava, 2011; Chakrabarti et al.,

2009; Assadi et al., 2012; Shirzad-Siboni et al., 2014; Liu et al., 2016). The high removal efficiency of Cr(VI) ions by ZnO photocatalysts was due to the high surface area of ZnO nanoparticles that responsible for absorbing positive metal ions in the wastewater. In addition, a few study also reported the use of ZnO as an adsorbent to remove several heavy metal ions such as Cu(II), Pb(II), Cd(II), Ni(II) (Wang et al., 2010a; Wang et al., 2013; Khan et al., 2013). Thus, the potential of ZnO nanomaterials in the removal of different heavy metal ions needs to be assessed.

Theoretically, removal of organic pollutants such as dyes by ZnO photocatalyst shall not affect the photocatalytic performance of ZnO particles in later stage. The organic pollutants shall decompose into less harmful by-products with smaller molecules such as water, carbon dioxide and less toxic substances. These by-products will carry away from ZnO photocatalyst by flowing water easily. In contrary, this is not the case for heavy metal ions removal by ZnO photocatalyst. The metal ions tend to deposit onto the surface of ZnO particles by photoreduction and absorption processes and form metals or metal oxides. Deposition and accumulation of these metals/metal oxides might affect the performance of ZnO photocatalyst in degrading the organic pollutants subsequently. It is worth to evaluate the heavy metal ions removal mechanism by ZnO photocatalyst and to assess its photodegradation efficiency on organic dyes in subsequent stage.

1.3 Research objectives

In this project, the reusability of ZnO particles in photodegradation of RhB dye after heavy metal deposition was studied. The following objectives were formulated in order to achieve the aim of this project:

- (i) To assess the photocatalytic activity of synthesized ZnO NRs and ZnO NDs via the degradation efficiency of RhB dye under UV and visible light illumination;
- (ii) To determine the removal efficiency of Cu(II), Pb(II), Ag(I), Cr(VI), Cd(II), Mn(II), Ni(II) ions by ZnO NRs;
- (iii) To evaluate the reusability of ZnO NRs in photodegradation efficiency of RhB dye after heavy metal deposition.

1.4 Scope of the study

This project is divided into 3 phases to achieve the objectives.

Phase 1: Synthesis and characterization of ZnO NRs and ZnO NDs.

Both ZnO NRs and NDs were synthesized by precipitation method. The ZnO NRs were fabricated by using zinc nitrate tetrahydrate ($\text{Zn}(\text{NO}_3)_2 \cdot 4\text{H}_2\text{O}$), 1,3-hexamethylenetetramine (HMTA, $\text{C}_6\text{H}_{12}\text{N}_4$) and polyvinylpyrrolidone (PVP, $(\text{C}_6\text{H}_9\text{NO})_n$). Whereas, zinc acetate dehydrate ($\text{Zn}(\text{CH}_3\text{COO})_2 \cdot 2\text{H}_2\text{O}$), aluminium sulphate ($\text{Al}_2(\text{SO}_4)_3$), ammonia hydroxide (NH_4OH) were used to synthesized ZnO NDs. Then, ZnO NRs and ZnO NDs were characterized by using Field Emission Scanning Electron Microscope/Energy Diffraction X-ray (FESEM/EDX), X-ray diffraction spectroscopy (XRD), High Resolution Transmission Electron Microscope (HRTEM).

The photocatalytic (PC) study of both ZnO nanoparticles were carried out via the degradation for Rhodamine B under UV and visible irradiation. The UV-Vis spectrometer was used to determine the degradation efficiency of RhB. Moreover, scavenger study was used to identify the main species which responsible for the decoloration of RhB dye as well as the photocatalytic mechanism of ZnO nanoparticles. The scavengers of hole (h^+), hydroxyl radical ($\cdot\text{OH}$) and superoxide

radical ($\cdot\text{O}_2^-$) were potassium iodide, methanol and benzoquinone, respectively. The purpose of this study was to select the ZnO particles with best PC for subsequent phases.

Phase 2: Removal of heavy metal ions by ZnO NRs

The removal of single element of heavy metal such as Ag(I), Cr(VI), Pb(II), Mn(II), Cu(II), Cd(II), and Ni(II) ions by ZnO NRs was studied. The initial concentration of heavy metal solution was 50 ppm which obtained by dissolving metal salts into deionized water. The concentration of metal ion at different time interval was measured by Inductively Coupled Plasma – Optical Emission Spectrometry (ICP-OES). Then the deposition of metal/metal oxide onto the surface of ZnO NRs (M/ZnO hybrid particles) was assessed by XRD, FESEM, HRTEM and EDX mapping.

Phase 3: Reusability of M/ZnO hybrid particles in the degradation of RhB dye.

The M/ZnO hybrid particles, which collected after heavy metal removal, was reused to investigate the photodegradation of RhB dye under exposure of UV and visible radiation. The degradation efficiency of RhB dye in the presence of M/ZnO was calculated via the intensity of UV-Vis absorption peak at 554 nm. The photocatalytic activity of M/ZnO hybrid particles was compared with ZnO NRs.

CHAPTER TWO

LITERATURE REVIEW

2.1 Water pollution

Depletion of fresh water resources is a global issue nowadays. There are many factors that lead to depletion of fresh water, including increase in population growth, climate change and water pollution due to dumping of industrial and domestic waste into water system without treatment. The water contamination includes many types of discharges such as organic dyes, heavy metals ions, pesticides and microbes. Approximately, water pollution causes 60,000 people die from diseases and 190 million people get ill each year (Jiang et al., 2012). According to study, 1 billion people are estimated lacking access to safe water supplies (Afroz & Rahman, 2017). Furthermore, 2.6 billion people in developing regions of Asia, Central and South America, and Africa are without access to basic sanitation (Alex Omo Ibadon & Fitzptrck, 2013).

Textile industry is one of the biggest sources of water pollution. The current wastewater treatment techniques are not able to remove easily toxic chemicals which have been identified from textile dyeing (Kant, 2012). In fact, the annual water use of the textile industry in China and European Union are 4 billion m³, 600 million m³ in 2016, respectively (WTO, 2016). Annually, 7x10⁵ tons of organic dyes are produced worldwide from the manufacturing and application processes. This shows a relationship between environmental issue and the clothing and textile manufacturers.

2.2 Organic dyes pollutants

2.2.1 Classification

Dyes are the abundant source of coloured organics arising as a waste from the textile industry. Dyes exhibit considerable structural diversity which comprises of two key components, i.e. chromophores and auxochromes. The chromophores delocalize electron with conjugated double bond, which is responsible for the unique color of dye. Whereas, the auxochromes intensify the colour of chromophores via electron withdrawing or electron donating substituent. Therefore, organic dye can be classified base on the structure of the chromophore such as azo dye, anthraquinone dyes, xanthene dye, nitro dye, acridine dye, triarylmethane dye.

Rhodamine B (RhB) is one of the most commonly dye used in the textile industry. It is also known as water tracer fluorescent for ground water tracking. The chromophores of RhB dye represent the electron system with conjugated double bonds like C=C, C=O and quinoid rings as shown in Figure 2.1. It is able to absorb a certain wavelength spectrum of visible light via the $n \rightarrow \pi$ transition of C=O, C=C groups. On the other hand, the auxochromes are functional groups of atoms attached to chromophores group such as hydroxyl (-OH) and amino (-NR) group. These functional groups do not absorb radiation itself in the visible range but has a shifting effect on main chromophore absorbance peaks or increasing their intensity (Chen et al., 2012).

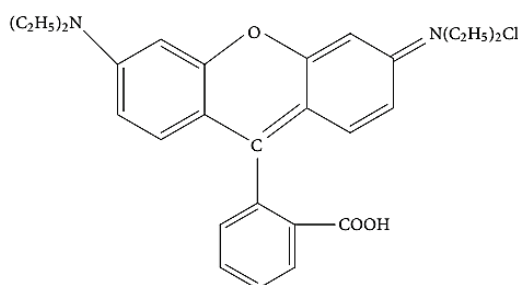


Figure 2.1 Structure of Rhodamine B (RhB) dye (Lam et al., 2012)

2.2.2 Impact of organic dye pollutants

The organic pollutants consist of dye, pesticide, pharmaceutical waste, which are dangerous to the ecological system and biological safety (Jiang et al., 2012). The textile, dyeing, pulp, paint industries and paper are the main consumers of dyes. Consequently, the wastewater from these industries usually contain high concentration of dyes. Organic dyes are considered toxic if entering human body via oral ingestion and inhalation. Some of the common syndromes are skin sensitization, skin and eye irritation (Christie, 2007). They impart colour to water and highly objectionable on grounds. RhB is a stable dye in natural condition, which is able to develop toxicity to humans as well as animals (Chen et al., 2012). Therefore, it is crucial to treat RhB dye before discharging into the river system.

2.2.3 Methods of dye removal

Normally industrial-wastewater treatment processes consists of pre-treatment, primary treatment, secondary treatment, tertiary treatment and final treatment (Hung et al., 2012). Firstly, the industrial organic wastes are pre-treated by using equalization and neutralization basin to accumulate pollutants.

The primary treatment is used to remove solid wastes by either physical or chemical separation techniques such as filtration and sedimentation. Filtration technology includes microfiltration, ultra-filtration and nanofiltration. Each filtration process depends on a particular contaminant that need to be treated (Cheremisinoff, 2001). The main drawbacks of filtration technique are high working pressures and a relatively short membrane life. The sedimentation is a physical process in which the suspended contaminants are settled by gravity using sedimentation basin. The

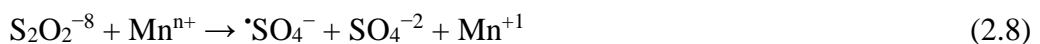
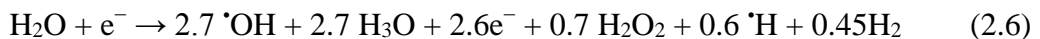
chemical flocculants e.g. aluminum (Al^{3+}), calcium (Ca^{2+}) or ferric (Fe^{3+}) ions are also used to enhance the flocculation dye effluent (Wang et al., 2006).

Biological treatment is commonly used as a secondary treatment in organic dye treatment (Hung et al., 2012). Number of bacteria are used for decomposition of dyes molecules. This method is cost-effective and complete mineralized of end product.

The pollutants that are not easily removed by biological methods then undergo the tertiary treatment. This treatment technique includes adsorption, electrochemical, chemical oxidation or advanced oxidation process (AOP). An adsorption technique is commonly applied for dyes removal. The adsorption is a process wherein a gas, liquid or dissolves solid is concentrated to a solid surface. This process bases on the chemical bonding or the Van der Waals forces between dyes molecules and the adsorbent surface (Gupta & Suhas, 2009). Alumina (Adak et al., 2005), silica gel (Phan et al., 2000) and activated carbon (Phan et al., 2006) are generally used as an adsorbent. Furthermore, low-cost adsorbents such as wood (Poots et al., 1978), coal (Mohan et al., 2002), fly ash (Lin et al., 2008) and sludge (Seredych & Bandosz, 2007) were also applied in removal organic dyes. However, the adsorbents after treatment become secondary pollutant and are not able to be reused for adsorbing the dyes.

Electrochemical technique is used as a tertiary treatment to remove organic pollutant. In this method, the electro-oxidation or electro-coagulation is used to degrade organic dyes (Gupta et al., 2007). In the electro-degradation of dyes, iron, boron doped diamond electrode etc., have been used as anode materials (Faouzi et al., 2007). The disadvantages of this technique are high cost and heavy metals production due to indirect oxidation (Gupta & Suhas, 2009).

Chemical oxidation is a method that dye effluent is treated via the utility of oxidizing agents. Oxidation process requires short reaction times and generally able to reduce molecular weight of organic compounds (Gupta & Suhas, 2009). AOP is known as the oxidation technique in which dyes are removed by the generated hydroxyl radicals ($\cdot\text{OH}$) and sulphate radicals ($\cdot\text{SO}_4^-$) (Deng & Zhao, 2015). These radicals are powerful oxidizing agents which decompose wastewater pollutants into less and even non-toxic products (Huang et al., 1993). Hydroxyl radicals are first generated by ozone (Eq. 2.1) (Gottschalk et al., 2009). Secondly, the $\cdot\text{OH}$ radicals are produced by semiconductor photocatalysts, such as titanium dioxide (TiO_2), zinc oxide (ZnO), zirconium dioxide (ZrO_2), cerium oxide (CeO_2), etc. (Eq. 2.2-2.3) (Tang, 2016). Thirdly, Fenton process (Eq. 2.4) (Pignatello et al., 2006), ultrasound irradiation (Eq. 2.5) and electronic-beam irradiation (Eq. 2.6) (Deng & Zhao, 2015) are also used to generate $\cdot\text{OH}$ radicals. On the other hand, sulphate radicals are formed by heat, ultraviolet (UV) irradiation (Eq. 2.7), transitional metals (Eq. 2.8) (Anipsitakis & Dionysiou, 2003).



The AOPs are potential and suitable for colour removal for many kind of dyes such as direct, reactive, vat and disperse (Gupta & Suhas, 2009). Nevertheless, AOPs process is pH dependent and producing undesirable by-products. Thus, the final step of organic dye treatment is the sludge processing and disposal.

2.3 Inorganic pollutants

2.3.1 Classification

The inorganic pollutants mainly consists of heavy metal, cyanide or nitrite. (Jiang et al., 2012). There are various reports in heavy metal pollutants which firstly classified on the removal of Copper (Cu), Chromium (Cr), Mercury (Hg), Lead (Pb), Cadmium (Cd) (Khalil et al., 2002; Rahimi et al., 2014; Wahyuni et al., 2015). Secondly, inorganic cyanide pollutant contains anion CN^- group, which is hazardous. The metallurgy, electroplating and other chemical industry are the main source of cyanide. The rapid development of metals industry leads to increase the emission of cyanide into the environment (Jiang et al., 2012). Finally, nitrite ion (NO_2^-) is known as a poisonous pollutant, which is able to cause illness and even cancer. Especially, it is not easy to remove the low concentration of NO_2^- due to its stability (Jin et al., 2001).

2.3.2 Impact of heavy metal pollutant

Heavy metals can be absorbed by sediment or fish when they are transferred into water environment. Silver particles are the ones most used in consumer product. It exists as a trace element in most metal ores and mineral. Silver is mainly come from iron and steel manufacturing, fossil fuel combustion and cement manufacturing (Eckelman & Graedel, 2007). Silver toxicity is not commonly considered as an environmental problem. However, silver is actually a toxic metal to human, which is

capable of causing haemorrhage, bone marrow suspension, heart and liver failure. In contrary, copper, lead, mercury, cadmium, nickel, chromium, manganese are common well-known toxic heavy metal which are a serious threat to people' health. For instance, the excessive ingestion of copper causes serious health issues such as convulsions, cramps, vomiting, or even death (Paulino et al., 2006).

Besides, exposure to mercury and lead may damage the circulatory system, nervous system, headache, dizziness, irritability, weakness of muscles (Barakat, 2011). Moreover, high concentrations of mercury could damage kidney function, dyspnoea and chest pain (Namasivayam & Kadirvelu, 1999). Cadmium and nickel have been known as a cancer-causing agent. Ingestion of cadmium and nickel result in kidney dysfunction, lung problems, skin dermatitis and even death at high levels of exposure (Borba et al., 2006). Chromium exists in the water environment mainly in two valence states, Cr(III) and Cr(VI). In general, Cr(VI) is more stable and toxic than Cr(III). Cr(VI) ion may accumulate in the food chain and lead to several health issues e.g. skin irritation and lung cancer (Khezami & Capart, 2005). Manganese is also essential for iron and steel production. The main effect of manganese occurs in the respiratory tract and brain. Thus, it is necessary to remove these toxic heavy metals contaminant to protect the people as well as the environment.

2.3.3 Methods of heavy metal removal

Nowadays, heavy metals pollutants are becoming more and more serious environmental issue. Several physical and chemical methods have been applied to solve this problem, including chemical precipitation (Ku and Jung, 2001), ion-exchange (Kang et al., 2004), adsorption (Fu & Wang, 2011), membrane filtration (Tortora et al., 2016) and photocatalytic process (Fu & Wang, 2011).

Recently, semiconductor photocatalytic process is the alternative process for wastewater treatment, especially for heavy metal removal. This photocatalytic process was achieved by the presence of semiconductor such as TiO_2 , ZnO , ZnS , CdS , CeO_2 , etc (Barakat, 2011). The photoinduced electrons are generated when the semiconductor is exposed under photon illumination. These carriers are capable of reducing heavy metal ions in solution depending on the reduction potential of metallic coupled. Generally, the photocatalytic performances with maximum reduction efficiency are obtained with TiO_2 (Barakat, 2011).

2.4 Semiconductor photocatalysis

The term photocatalysis is known as a phenomenon that connecting both photochemistry and catalysis (Anandan et al., 2010b). According to International Union of Pure and Applied Chemistry, photocatalysis is defined as the change in the rate of chemical reaction under the action of photons radiation in the present of a photocatalyst (Kisch, 2014; Braslavsky et al., 2011). Semiconductor photocatalysis consists of wide band gap semiconductor (TiO_2 , ZnO , SnO_2 , ZrO_2 , ZnS , etc.) and narrow band gap semiconductor (Fe_2O_3 , WO_3 , CdS , CdSe , etc.) which are shown in Figure 2.2.

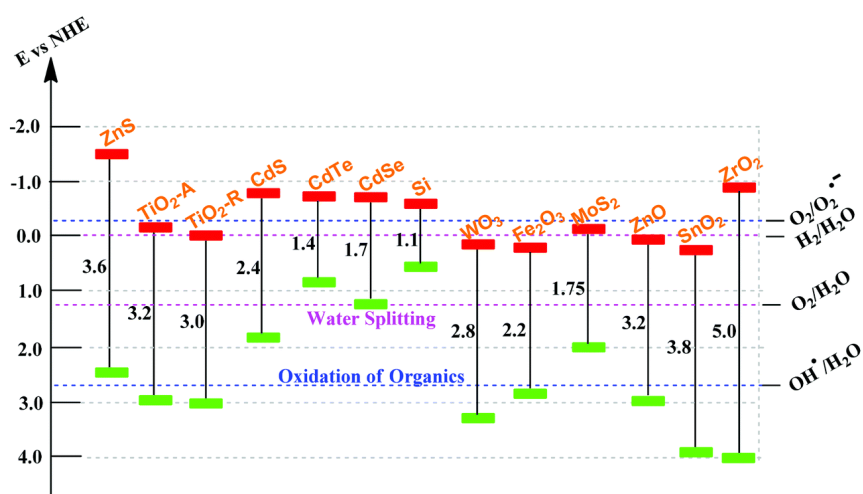


Figure 2.2 Band gap energy, VB and CB for a range of semiconductors on a potential scale (V) versus the normal hydrogen electrode (NHE) (Wu et al., 2015).

2.4.1 Applications

2.4.1.1 Photocatalytic degradation of organic dye pollutants

Most textile dyes pollutants are stable, thus make them resistant towards decomposition by biochemical and physical-chemical treatment method (Arslan & Balcioglu, 2001). Recent years, photocatalysis method has been widely used in the removal of organic dyes due to its ability to completely mineralize the organic pollutants (Chakrabarti & Dutta, 2004; Reddy et al., 2007; Akpan & Hameed, 2009). Semiconductors photocatalysts e.g. TiO_2 , ZnO , WO_3 , Fe_2O_3 , ZrO_2 and CdS have been studied for the degradation of organic dyes.

TiO_2 photocatalyst is able to degrade a wide variety of organic pollutants like dye wastewater (Asiri et al., 2011), pharmaceutical wastewater (Elmolla & Chaudhuri, 2010), pesticide wastewater (Sharma et al., 2008; Wu et al., 2010). On the other hand, ZnO photocatalyst has been proven as a potential candidate for treatment organic dyes exposure to UV and visible radiation (Lee et al., 2016). For instance, ZnO is used to remove Acid Red 18 (Sobana & Swaminathan, 2007), Methylene Blue (Danwittayakul et al., 2015), Methyl Orange (Xie et al., 2011), Acridine Orange (Pare et al., 2008), Orange II (Siuleiman et al., 2014). Photocatalytic performance of TiO_2 , ZnO , CdS and SnO_2 were investigated via the photodegradation of Methyl Orange and Rhodamine 6G (Kansal et al., 2007). The ZnO was found to be higher photocatalytic activity than the others, particularly TiO_2 . Whereas, the recombination of electron-hole pairs reduced the activity narrow band gap semiconductor CdS . While, SnO_2 is not excited due to its wide band gap, consequencely low removal efficiency.

The applications of ZnO photocatalyst in organic dyes degradation were summarized in Table 2.1. It can be seen that the photocatalytic activity of ZnO is not

only sensitive to the excitation source, pH of solution, size of catalyst but also the morphology. ZnO photocatalyst with different morphologies performed different efficiency in degradation of various types of organic dyes under UV irradiation. The active site on the surface of ZnO affects the photocatalytic reaction at the liquid interface between catalyst and organic compound. Therefore, the photocatalytic of ZnO NRs and ZnO NDs was evaluated in this current work.

Photocatalytic degradation of RhB dye using ZnO photocatalyst has been widely studied (Thein et al., 2015a; Thein et al., 2015b; Rahman et al., 2013; Nagaraja et al., 2012; Seo & Shin, 2015). Photoinduced self-sensitized photolysis of RhB without using stacked ZnO nanorods is minimal as the characteristic peak of RhB (533 nm) reduced about 10 % after 60 min UV illumination (Thein et al., 2015b). Base on the study of Thien et al (Thein et al., 2015b), the enhanced photocatalytic activities with the present of stacked ZnO nanorods was significant. Figure 2.3 showed that the absorption peak of RhB decreased as a function of irradiation time. The degradation efficiency of RhB dye was proximately 98.7 % after 75 min of UV irradiation.

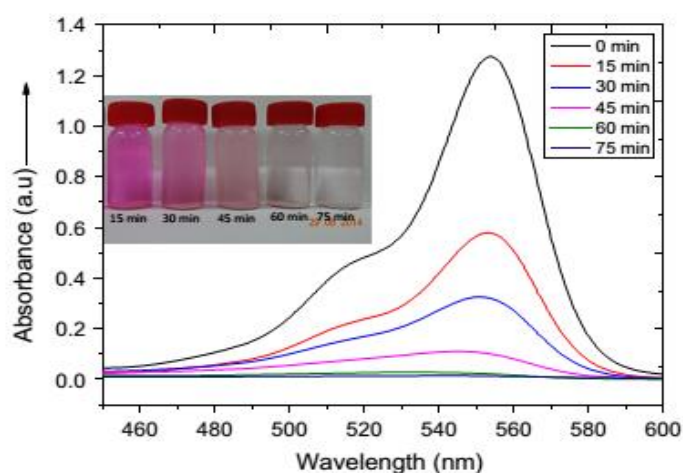


Figure 2.3 Absorbance spectra of RhB solution degraded by stacked ZnO nanorods under UV light irradiation (Thein et al., 2015b)

In the photocatalytic process, reactive species like holes (h^+), electron (e^-), hydroxyl radicals ($\cdot OH$) and superoxide anion radicals ($\cdot O_2^-$) can be generated by the interactions between ZnO photocatalyst and optical excitation light source. One or more of these ROSs generated could be responsible for the degradation of RhB dye. In order to identify the dominant ROS(s) that responsible for the degradation of RhB dye and to deduce the photodegradation mechanism, scavenger tests were performed.

Different scavenger agents were used i.e. benzoquinone (BQ), methanol (ME) and potassium iodide (KI). BQ can be used to detect the superoxide anion ($\cdot O_2^-$) due to their ability to trap this ion radical by an electron transfer mechanism as shown in Eq. 2.9 (Palominos et al., 2009). The presence of KI from a solution provides iodide ion as a scavenger, which reacts with h^+ (Eq. 2.10). KI can be used to identify the involvement of hole in the direct oxidation of organic substrate (Palominos et al., 2009). On the other hand, ME is known as an efficient scavenger of free or adsorbed $\cdot OH$ radicals as well as h^+ scavenger (El-Morsi et al., 2000). It is also noted that electron does not contribute directly to the degradation of organic dye (El-Morsi et al., 2000; Liu et al., 2013). Thus, the effectiveness of e^- was not study in this project.



Table 2.1 Photodegradation of organic dyes in aqueous solution of ZnO particles.

Catalyst, size	Catalyst loading (g/l)	Pollutant, concentration	Irradiation time (min)	pH	Excitation wavelength (nm)	Degradation efficiency (%)	Degradation rate (min ⁻¹)	Reference
ZnO nanorod 525 nm	1	Methylene Orange 20 ppm, 100 ml	120	-	365	100	-	(Xie et al., 2011)
ZnO, 100 nm nanowire	0.5	Orange II 10 ppm, 250 ml	60	-	315-400	100	-	(Siuleiman et al., 2014)
CdS/Ag/ZnO 6.4 nm	2	Reactive Orange 4 Reactive Yellow 84 5 ppm, 50 ml	50 50	7	Solar light	100 100	-	(Subash et al., 2016)
ZnO, 5 m ² /g commercial	1.5	Remazol Red F3B 150 ppm, 100 ml	60	7	365	100	-	(Akyol & Bayramoğlu, 2005)
ZnO nanorod 0.1-4 µm	4	Acid Red 18 5 ppm, 400 ml	120	7	365	99	0.036	(Sobana & Swaminathan, 2007)
ZnO, 5 m ² /g commercial	0.25 - 2	Methylene Orange Rhodamine 6G 5-200 ppm	90 30	4 10	Solar light	99 91	0.017 0.016	(Kansal et al., 2007)
Cu/ZnO, Ball, 40 nm	3	Direct Blue 71 10 ppm, 100 ml	120	7	400-780	98	0.052	(Thennarasu & Sivasamy, 2016)
ZnO, 100 nm nanonails	1	Crystal Violet 10 ppm, 100 ml	70	-	365	95	-	(Tripathy et al., 2017)
ZnO, 25 nm nanospherical	0.1	Methylene Orange 5 ppm, 150 ml	120	-	365	90	-	(Goudarzi et al., 2017)
ZnO nanorod 20-30 nm	1.2	Rhodamine B Butyl Rhodamine 2.5 ppm, 50 ml	100	6-7	400	76 75	0.012 0.015	(Yu et al., 2004)

The narrow band gap WO_3 semiconductor catalyst was studied for the degradation of Acid Red 87 dye (Qamar et al., 2009). The Acid Red 87 dye was completely degraded within 12 minutes under laser irradiation instead of UV lamp. On other study, the WO_3 nanoparticles were synthesized by precipitation method and utilized as photocatalyst for removal of methylene blue under visible light illumination (Rahimi et al., 2017). The degradation efficiency was found to be 90 % after 1 hour of irradiation. Furthermore, Bharadwaj and coworker reported that Congo Red dye was degraded 98 % using Fe_2O_3 photocatalyst at pH 4 within 4 hours irradiation of sunlight (Bharadwaj et al., 2012). However, after a photodegradation process, Fe_2O_3 needs to be accompanied with a secondary treatment.

In the semiconductor photocatalytic process, organic dyes are able to be mineralized completely into CO_2 and H_2O under photo excitation. The photocatalytic reactions occurs when ZnO particles absorbs the energy that larger than its band gap energy. Then, photoinduced electrons are promoted from the VB to the CB, generating positively hole (h^+_{VB}) and electron (e^-_{CB}) (Eq. 2.11). The “hot” electrons typically relax to the edge of CB very rapidly. These electrons also can be diffused to the surface of ZnO and react with the surrounding or recombine via bulk state (Eq. 2.12). During a time of ~ 100 femtoseconds, these electrons may get trapped and react with the surrounding or recombine in surface state. The dissolved oxygen acts as electron acceptor that extend the recombination of electron-hole pairs and form the superoxide radicals, $\cdot\text{O}_2^-$ (Eq. 2.13). The h^+_{VB} can also migrate through the surface of ZnO and react with OH^- leads to the formation of hydroxyl radicals ($\cdot\text{OH}$) (Eq. 2.14). The $\cdot\text{OH}$ radical is an extremely strong, non-selective oxidant which leads to the complete mineralization of organic dyes (Eq. 2.15). Moreover, the electron tranfer from organic dyes to h^+_{VB} allows the direct oxidation of dyes into

intermediates substance (Eq. 2.16). The $\cdot\text{O}_2^-$ radicals were further protonated to form hydroperoxyl radical ($\cdot\text{HOO}$) and subsequently H_2O_2 (Eq. 2.17-2.19). The $\cdot\text{HOO}$ radicals are able to trap e^-_{CB} which further enhance the photocatalytic activity (Lee et al., 2016).

Table 2.2 Photodegradation mechanism of dyes pollutant under UV and visible light (Zhao et al., 2005; Chen et al., 2010)

UV illumination		Visible light illumination	
$\text{ZnO} + h\nu \rightarrow \text{ZnO}$	(2.11)	$\text{Dye} + h \rightarrow \text{Dye}^*$	(2.20)
$e^-_{\text{CB}} + h^+_{\text{VB}} \rightarrow \text{phonon or photon}$	(2.12)	$\text{Dye}^* \rightarrow \text{Dye}^+ + e^-$	(2.21)
$e^-_{\text{CB}} + \text{O}_2 \rightarrow \cdot\text{O}_2^-$	(2.13)	$\text{ZnO} + e^- \rightarrow \cdot\text{ZnO}^-$	(2.22)
$h^+_{\text{VB}} + \text{OH}^- \rightarrow \cdot\text{OH}$	(2.14)	$\cdot\text{ZnO}^- + \text{O}_2 \rightarrow \text{ZnO} + \cdot\text{O}_2^-$	(2.23)
$\cdot\text{OH} + \text{R-H} \rightarrow \text{R}^{\cdot*} + \text{H}_2\text{O}$	(2.15)	$\cdot\text{O}_2^- + \text{H}_2\text{O} + e^- \rightarrow 2\text{H}_2\text{O}_2$	(2.24)
$h^+_{\text{VB}} + \text{R} \rightarrow \text{R}^{\cdot*} \rightarrow \text{Intermediates}$	(2.16)	$\text{H}_2\text{O}_2 + e^- \rightarrow \cdot\text{OH} + \text{OH}^-$	(2.25)
$\cdot\text{O}_2^- + \text{H}^+ \rightarrow \cdot\text{HOO} + \cdot\text{O}_2^- \rightarrow \cdot\text{HOO} + \text{O}^-$	(2.17)		
$\cdot\text{HOO} \rightarrow \text{H}_2\text{O}_2 + \text{O}_2$	(2.18)		
$\text{H}_2\text{O}_2 + \cdot\text{O}_2^- \rightarrow \cdot\text{OH} + \text{OH}^- + \text{O}_2$	(2.19)		

Due to a wide band gap semiconductor, the photocatalytic performance of ZnO under visible light irradiation is much different from that under UV radiation. The major differences in mechanism are shown in Figure 2.4 and Table 2.2 (Zhao et al., 2005). In this process, the photon does not excite directly ZnO semiconductor. Instead, the dye molecules absorb visible light and become excited state (Eq. 2.20). This excited dye (Dye^*) injects electrons to the CB of ZnO in Eq. 2.21-2.22. These injected electrons on the CB can reduce the dissolved oxygen to produce the oxidizing species e.g. H_2O_2 , $\cdot\text{O}_2^-$ and $\cdot\text{OH}$ radicals (Eq. 2.23-2.25). These active radicals are responsible for the degradation of dye molecule (Pare et al., 2008). It is noted that only organic species which can be excited by visible light are degradable with the presence of semiconductor photocatalyst (Zhao et al., 2005). In addition, the mineralization process usually takes longer time than under UV light.

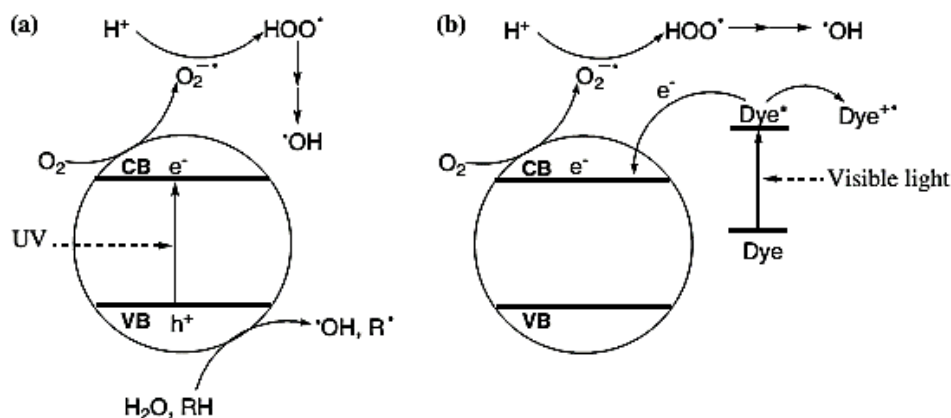


Figure 2.4 The photocatalytic mechanism of organic dye degradation under (a) UV and (b) visible light illumination (Zhao et al., 2005).

2.4.1.2 Photocatalytic removal of heavy metal pollutants

Nowadays, photocatalytic process in aqueous suspension of semiconductor (TiO_2 , ZnO , CdS , WO_3 , ZnS) has not only received attention in the degradation of dye pollutants but also in the removal of inorganic pollutants (Barakat, 2011). Among these semiconductors, the investigation of TiO_2 has been widely employed for various heavy metal ion such as $Cd(II)$, $Pb(II)$, $Cr(VI)$, $Cu(II)$, $Hg(II)$, etc. (Guan et al., 2012; Wahyuni et al., 2015; Khalil et al., 2002; Song, 2003). For instance, the removal of $Cr(VI)$, $Cu(II)$, $Pb(II)$ and $Cd(II)$ ions in aqueous suspension of TiO_2 were 78.72 %, 45.56 %, 40.32 % and 15.23 %, respectively after 24 hours at pH 5 (Wahyuni et al., 2015).

Beside, ZnO nanoparticles (NPs) have been widely using in heavy metal removal. The structure, morphology and properties of ZnO NPs can be tailored to serve specific application. In fact, ZnO NPs with different morphology have been synthesized and used for the photoreduction of $Cr(IV)$ in an aqueous medium under solar radiation. The results indicated that the double reduction efficiency was obtained as compared to commercial ZnO microparticles (Banerjee et al., 2012b). Furthermore, ZnO photocatalyst was also applied to remove $Pb(II)$ (Lee et al., 2006) and $Ni(II)$

(Shirzad Siboni et al., 2011). Besides, many narrow band gap semiconductor catalysts, such as WO_3 (Yang et al., 2010), CuO (Yu et al., 2015) and CdS (Wang et al., 1992) have been investigated for the photoreduction of Cr(VI) to Cr(III) . Table 2.3 showed the photocatalytic removal of heavy metal pollutants by various semiconductor photocatalysts. Mostly, ZnO photocatalyst was used to reduce Cr(VI) under UV light illumination. The removal efficiency of Cr(VI) ion was improved by increasing the energy of excitation source or the irradiation duration. Furthermore, the removal of heavy metal ions is sensitive to the pH level of the solution.

The photocatalytic removal mechanism of heavy metals ion in wastewater usually bases on photocatalytic reduction and oxidation (Wahyuni et al., 2015; Shirzad Siboni et al., 2011; Yang & Chan, 2009). These reactions are induced by UV light and sensitized by semiconductor photocatalyst (Wahyuni et al., 2015). TiO_2 was chosen to demonstrate the mechanism of photocatalytic removal of inorganic pollutants. Electron-hole pairs are produced when TiO_2 is excited by photon which is equal or greater than its band gap energy (Eq. 2.26) (Jiang et al., 2012). In the absence of electron acceptor, the recombine of electron-hole pairs happens in <100 nanosecond. Electron acceptors (A) can be reduced by e^-_{CB} , while donor species (D) can give electrons to holes, being oxidized as shown in Eq. 2.27-2.28 (Litter, 2015).



Figure 2.5 shows the band edges position of ZnO versus redox potentials of various metallic couples and oxidation potentials of water. The theory describes that the reduction reaction occurs when potential of metallic couples (Cd^{2+}/Cd , Ni^{2+}/Ni ,

Pb^{2+}/Pb , Cu^{2+}/Cu , $\text{Cr}_2\text{O}_7^{2-}/\text{Cr}_3^+$, etc.) is more positive than the e^-_{CB} level. While redox potentials is less positive than the h^+_{VB} level can permit the oxidation reaction. Figure 2.2 highlights the energy band gap of different semiconductor photocatalyst with the energy levels of the e^-_{CB} and the h^+_{VB} . Furthermore, Guan et al. (Guan et al., 2012) illustrated that TiO_2 acts as photocatalyst to oxidize As(III) to As(V) then adsorbs As(V) ion in the presence of UV light or sunlight irradiation. However, it works only as adsorbent in the absence of irradiation as shown in Figure 2.6.

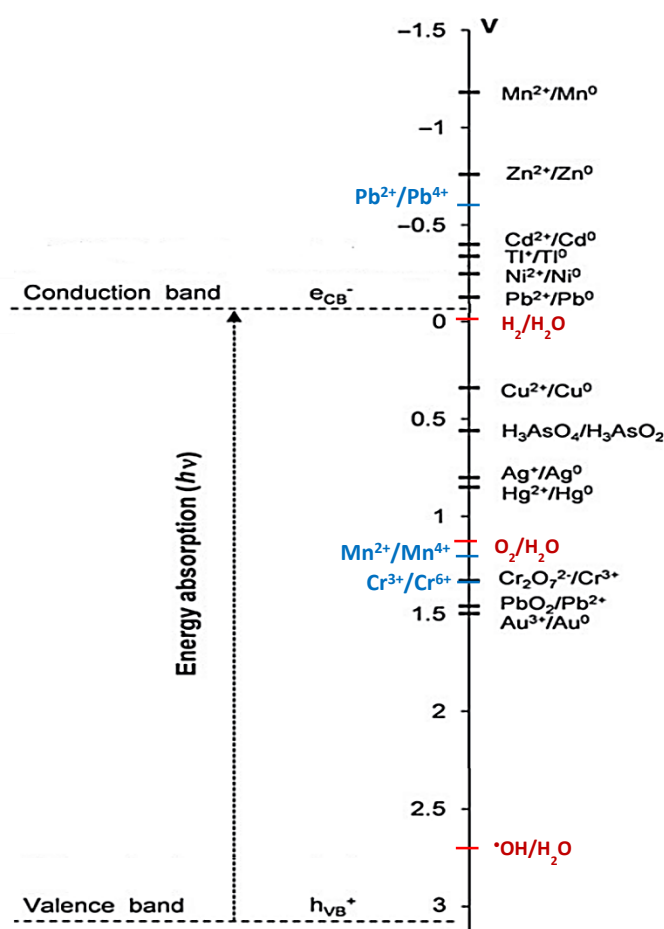


Figure 2.5 Position of the redox potentials of various metallic couples and oxidation potentials of water related to the energy levels vs. NHE of ZnO photocatalyst (Wang et al., 2010b; Litter, 2015; Vanysek, 1998).

Table 2.3 Heavy metal removal using semiconductor photocatalysts.

Catalyst Size (nm)	Catalyst loading (g/l)	Pollutant	Pollutant concentration (ppm)	Irradiation time (min)	pH	Excitation wavelength, (nm)	Removal efficiency (%)	Reference
TiO ₂ , P25	1	As(III)	50	60	7	365	100	(Ferguson et al., 2005)
TiO ₂ , 21 Particle	0.9	Pb(II) Cd(II)	25	56	11	254	93 88	(Rahimi et al., 2014)
TiO ₂ , 500 μm	5	As (II)	50	180	3	365	80	(Zhang & Itoh, 2006)
ZnO, 30	3	Cu(II)	52	90	-	400	100	(Lee et al., 2008)
ZnO, nanosized	3	Pb(II) Cu(II)	150 52	30 80	7	365	100	(Lee et al., 2006)
ZnO, 10 to 70	1	Cr(VI)	75	60	7	355	95	(Qamar et al., 2011)
ZnO, 50 Particle	1	Ni(II) Cr(VI)	20	120 120	7 7	247	90 80	(Shirzad Siboni et al., 2011)
ZnO, 87 ZnS, 190 CdS, 80 ZrO ₂ , 68	20	Cr(VI)	200	120	7	365	85 85 50 50	(Karunakaran et al., 2009)
ZnO, 6 to 12	0.15	Cr(VI)	0.5	15	4-5	366	83	(Assadi et al., 2012)
ZnO, 20 to 100 CdS, nanosized	5	Cr(VI)	50	180	2	350-400	78 49	(Joshi & Shrivastava, 2011)
ZnO, 20-50	1	Cr(VI)	20	360	7	400-700	68	(Yang & Chan, 2009)
ZnO, 28 to 150	0.4	Cr(VI)	50	120	6.6-6.9	Solar light	35	(Banerjee et al., 2012a)